Molecular Crystals and Liquid Crystals

Publication details, including instructions for authors and subscription information:
http://www.tandfonline.com/loi/gmcl20

Towards 3D metal-dielectric photonic crystal. Optical characterization

P.-T. Miclea [a], S. G. Romanov [a], C. M. Torres [a], Z. Liang [b], A. Susha [b] & F. Caruso [b]

[a] Department of Electrical and Information Engineering, Institute of Materials Science, Wuppertal, Germany

[b] Max Planck Institute of Colloids and Interfaces, Potsdam, Germany

Version of record first published: 18 Oct 2010

To cite this article: P.-T. Miclea, S. G. Romanov, C. M. Torres, Z. Liang, A. Susha & F. Caruso (2004): Towards 3D metal-dielectric photonic crystal. Optical characterization, Molecular Crystals and Liquid Crystals, 415:1, 211-219

To link to this article: http://dx.doi.org/10.1080/15421400490481197

Mol. Cryst. Liq. Cryst., Vol. 415, pp. 211–219, 2004

ISSN: 1542-1406 print/1563-5287 online
DOI: 10.1080/15421400490481197

Taylor & Francis
Taylor & Francis Group

TOWARDS 3D METAL-DIELECTRIC PHOTONIC CRYSTAL. OPTICAL CHARACTERIZATION

P.-T. Miclea, S. G. Romanov, and C. M. Sotomayor Torres
Institute of Materials Science, Department of Electrical and Information Engineering, University of Wuppertal, D-42097, Wuppertal, Germany

Z. Liang, A. Susha, and F. Caruso
Max Planck Institute of Colloids and Interfaces, D-14424, Potsdam, Germany

The interaction between surface plasmon resonance of the metallodielectric photonic crystal and the Bragg resonance of the opal photonic crystal has been studied. Two types of samples were investigated, differing in the topology of the metal content, metal-dielectric photonic crystals prepared using layer-by-layer deposition coating spheres with oppositely charged polyelectrolyte and Au nanoparticles and infiltrated opaline structures with Au nanoparticles. It was found that when the "red" -shift of plasmon resonance overlaps the Bragg diffraction, the latter become almost disperionless.

INTRODUCTION

Three-dimensional (3D) photonic crystals (PhCs) lend themselves to modify and study fundamental optical properties as refraction, localization and the emission rate of light. 3D PhCs colloidal crystals and their derivatives, like inverted opals has been investigated recently, however, the fixed symmetry of opals and the limited choice of high dielectric constant semiconductors make it difficult to obtain a wide and robust full photonic bandgap (PBG) [1]. An alternative way is to realize an opal-like structure

Received 10 June 2003; accepted 18 August 2003.

We are grateful to Mr. D. N. Chigrin for the photonic band-structure calculations and for valuable discussion. This work was supported by EU-IST-2001-38195 Funlight Project and DFG Framework Program Photonic Crystals.

Address correspondence to P.-T. Miclea, Institute of Materials Science, Dept. of Electrical and Information Engineering, University of Wuppertal, Wuppertal, D-42097, Germany.

from metal spheres, which changes dramatically the light dispersion inside the PhC and results in the opening of a full PBG [2,3]. So far, the preparation of opals from submicrometer metal spheres has not been reported. It is well known that in metal particles have different optical properties in the visible range, such as the complex dielectric function if their size is in the nanometer scale. To study of these properties combined with the properties of opal photonic crystals, one approach is to cover the dielectric core with a metallic shell obtaining a core-shell structure [4]. In this case the optical properties of the complex system are given by the properties of the opal structure superimposed with the influence of the metal nanoparticles. However the assembly of metal-dielectric (MD) core-shell spheres is a complex task, which was solved only recently [5]. In this paper we show and discuss the influence of the Au nanoparticles distribution and topology on the reflectance spectra of the metallodielectric photonic crystal.

EXPERIMENTAL

Polystyrene (PS) spheres of diameter $D = 640$ nm were coated with eight layers of negatively charged polyelectrolyte in order to incorporate a certain amount of Au nanoparticles (NP) in them from positively charged 4-dimethylaminopyridine-stabilized Au. TEM analysis shows that the Au NCs possess a narrow size distribution centered around 5 nm [6]. Two types of opal thin films were studied. One set denote samples T1, which were prepared by first impregnating the polyelectrolyte coated spheres with 5 nm Au NPs to form the core-shell structures and then assembling them in face centered cubic (fcc) lattice [6], as shown in Figure 1(a). The other sample set T2 were made by first assembling the polyelectrolyte coated-spheres in to an opaline structure and then infiltrating with Au NPs as schematically presented in Figure 1(b). SEM micrograph of T1 MD opal is shown in Figure 2. The estimated film thickness is about 12 nm. Sphere diameters of these MD opals were obtained from surface diffraction measurements as 595 and 660 nm in T1 and T2 opals, respectively. From thermogravimetric analysis (TGA) measurements the gold content was determined to be 3.4 and 5.8 wt.% for the T1 and the T2 opals, respectively.

Probing the Au content by electron probe microanalysis (EDX) using as prepared and cleaved samples shows that the Au Lα line (2.71 keV) is 18% more intense in T2 than in T1 opal and the Mα line is weaker by the same proportion. This could be interpreted by assuming that in T1 opals the Au nanoparticles are uniform distributed in the sample and that in the T2 samples particles aggregates in the voids of the opal. This would explain

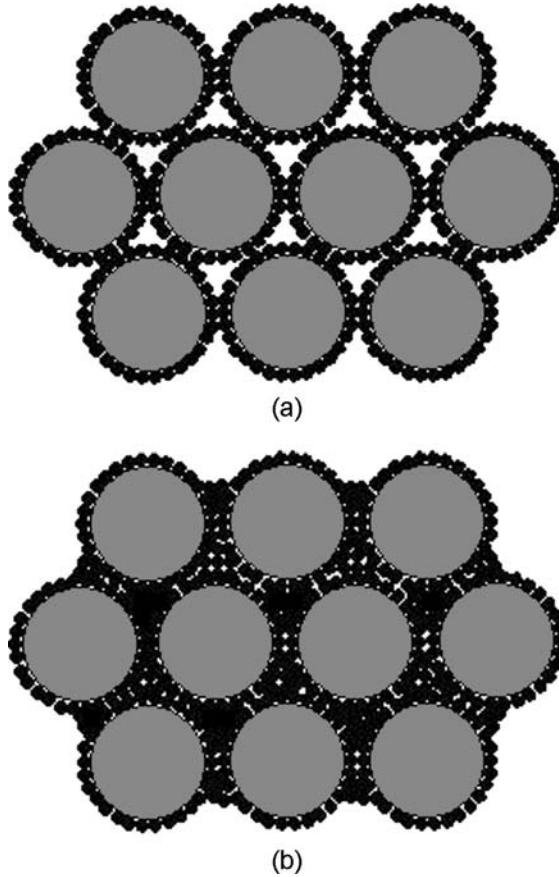

FIGURE 1 Schematics of metallodielectric photonic crystals made using layer-by-layer deposition of core-shell structures here called T1, (a) and impregnation (b) of PS spheres with Au nanoparticles, sample T2.

the decrease of the Mα line generated by the particles in T2 opals would be absorbed by neighboring particles. Likewise, if in T1 opals we assume a uniform coverage of PS spheres with Au NPs, whereas in T2 opals the NPs density depends on the void topology.

Angle-resolve reflectance spectra of both samples were recorded in the visible and near-infrared ranges. The samples were illuminated by a collimated beam of white light from a halogen tungsten lamp with 1 mm spot diameter. An aperture was used to select the reflected light within 5° solid angle along directions identified by the angle θ with respect to the [111] axis of opal lattice.

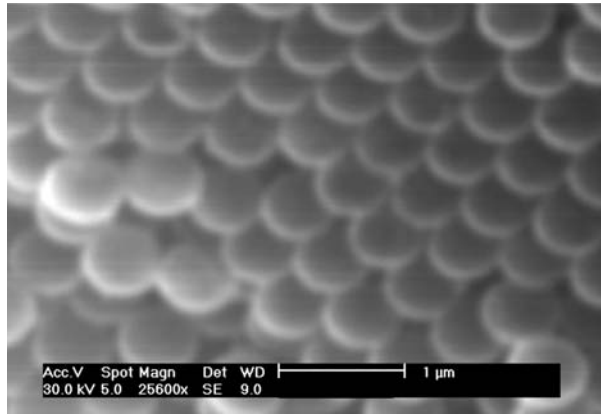

FIGURE 2 SEM micrograph of a typical T1 Au/PS opal structure.

RESULTS AND DISCUSSION

Band structure calculations using plane waves show that the $\Gamma-\mathrm{L}$ bandgap of bare PS opals is centered at 1370 nm for spheres of 640 nm diameter presented in Figure 3. On the other hand Zhang *et al.* [3,7] shows that in the case of metal spheres with a diameter of 160 nm the band-gap is at 900 nm. Reflectance spectra of T1 and T2 Au/PS opals are shown in Figure 4 for an angle of incidence $\theta = 25^{\circ}$. In both cases the surface plasmon resonance of isolated Au NPs at 570 nm is observed. Using the Mie theory [8], in the quasistatic approximation, for Au nanoparticles with a mean size of 10 nm on a dielectric surface the resonance position is centred at 530 nm. The second common feature is the diffraction resonance of the opal lattice. In T1 Au/PS opal the Bragg resonance appears at 1350 nm for $\theta = 20^{\circ}$ (Fig. 4 solid line). In the Figure 5 the angular dispersion of this peak is shown together with the Bragg law fit:

$$\lambda_{hkl} = 2d_{hkl}\sqrt{n^2 - \cos^2(r_{hkl})} \tag{1}$$

where $d_{hkl} = 0.816D$ is the distance between (111) planes, r_{hkl} is the internal angle between the wavevector and the [111] direction and n is the refractive index (RI). From the position of the Bragg diffraction resonance a sphere diameter of 570 nm is obtained, which is within 5% of the value obtained using surface diffraction.

The T1 Au/PS opal shows an intensive band centered at 770 nm (Figure 6). This peak is angle-independent in the θ range 0°–35°. When $\theta > 30^{\circ}$, another maximum appears at 670 nm. A further increase of θ

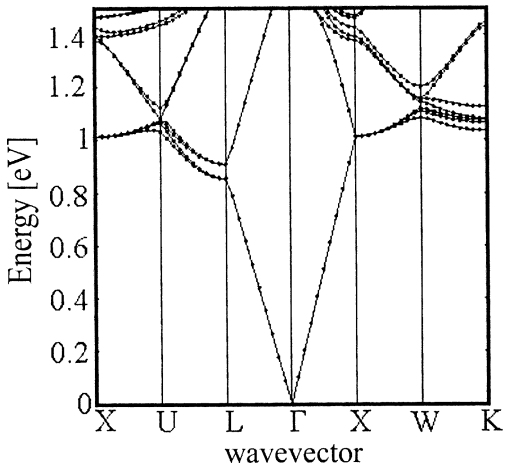

FIGURE 3 Calculated band structure of uncoated PS spheres with a diameter of 640 nm.

results in a more intense 670 nm peak and a weaker intensity 770 nm peak. The latter is no longer observed for $\theta \geq 55°$.

To interpret this behavior we assume that the shell in T1 Au/PS opals is made from well separated and, ideally, non-interacting Au NPs. However, when the spheres are assembled in a close packed lattice, fragments of

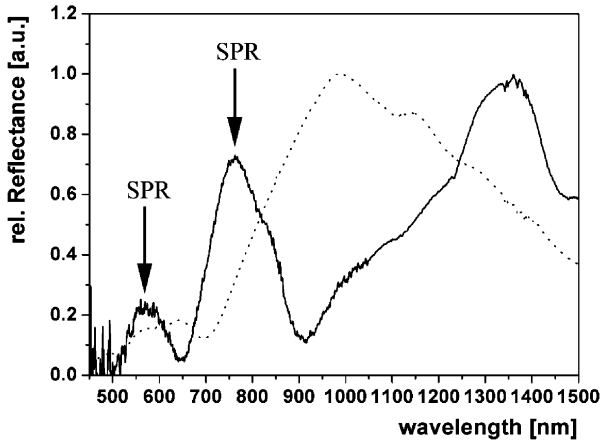

FIGURE 4 Angle-resolved reflectance spectra of the T1 Au/PS opal (solid line) and T2 Au/PS opal (doted line). The spectra were collected at an incidence angle of 25°.

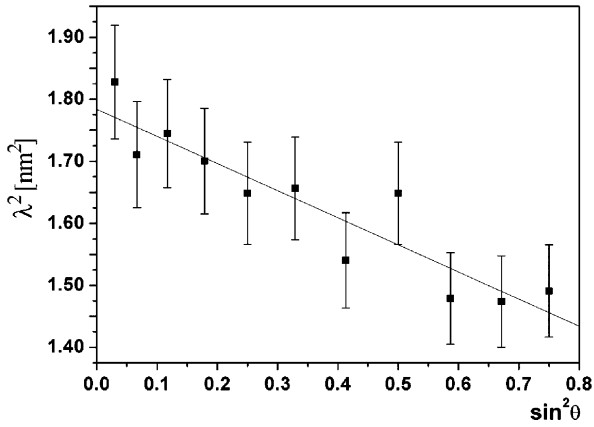

FIGURE 5 Angular dispersion of the Bragg resonance in T1 Au/PS opal. Error bars correspond to 5% uncertainty in the peak central wavelength. The solid line represents the calculated Bragg dispersion for a bare opal of PS spheres of 640 nm diameter.

sphere surfaces form the faces of polyhedrons, which approximate the shapes of opal voids [9]. In a fcc lattice the free space can be represented as a lattice of octahedral (O) and tetrahedral (T) voids multiply-connected via narrow channels (C), the characteristic sizes of which are $d_O = 0.41D$, $d_T = 0.23D, d_C = 0.15D$, respectively. At the polyhedra edges the

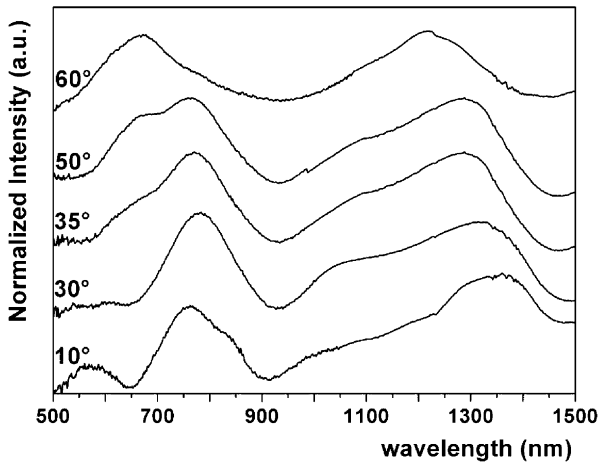

FIGURE 6 Reflectance spectra of the T1 Au/PS opal. Spectra are shifted vertically for clarity.

thickness of NP-embedded layers doubles and as expected, with decreasing void size the volume of high NP density increases. Therefore, the highest local density can be expected in channels and at points where the spheres touch. Because the polyelectrolyte layers are loose and soft, they can also be compressed leadings to NP aggregation. Due to the lattice arrangement of spheres, Au NP aggregates are shaped in lines which, in turn, are regularly oriented in the opal space. Being part of the lattice, evidence of the presence of these elongated aggregates could be seen at different angles by changing the angle of light incidence θ. Since the resonance frequency of the surface plasmon is split for elongated NPs [10,11], the interplay of the 650 nm and 750 nm bands could be attributed to ordered arrangement of Au NP aggregates. The broadening of resonance maxima in our samples is due to the high symmetry of fcc lattice, which results in a multiple choice of linear aggregate projections on the detection direction.

In T2 Au/PS opals the density of Au NPs in the shell layer is larger than in the T1 Au/PS opal and polyhedra shapes are expected to be smeared out because the infiltration homogeneity is affected by opal packaging. Thus, the probability of aggregation increases, but the aggregates acquire irregular shapes leading to poorly resolved plasmon resonances at 570 nm and 650 nm and a large "red" shifted background. The reflectance spectrum (Fig. 4 dashed line) also shows a broad maximum centered at about 950 nm with a shoulder peak of lower intensity at 1130 nm.

The "red" shifted plasmon resonance in T2 Au/PS opal overlaps with the Bragg resonance along [111] axis of the opal. This overlap changes dramatically the diffraction properties of Au/PS-NP/opal. A plot of λ^2 as a function of $\sin^2(\theta)$(Fig. 7) shows the dispersion linearised but with the slope sign opposite to the case of bare PS opals (cf Fig. 5).

The band structure of polymer opal shows that the decrease of the L-gap central wavelength along changing the wavevector from $\Gamma-\mathrm{L}$ to $\Gamma-\mathrm{U}$ direction [11], which would explain the "blue" shift of the Bragg resonance when deviating from the [111] direction. It is reasonably to assume that the deviation of the Au/PS-opal angular dispersion from the Bragg law is caused by the strong variation of the RI with wavelength. To explore the validity of this assumption we calculate the shift of the resonance using the Mie theory. The dielectric function of the bulk Au was taken from [12] and corrected for the small size of the Au NP (see, e.g. ref. [10] and references therein). As discussed above in the T2 opal sample the metal particles cover the walls of the voids in such a way that we can consider these voids as core-shell particles with an air core and metal NPs forming the shell. The calculations take these core-shell particles in consideration. We consider the volume of the core-shell equal to the volume of the voids and the shell thickness to be about 20 nm. From the Mie theory it is well known that the resonance position red shifts by (i) increasing the shell

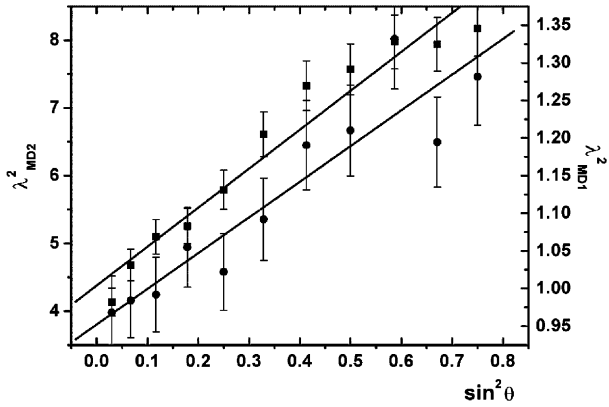

FIGURE 7 Angular dispersion of the bands centred at 1025 nm (left scale, squares) and 1300 nm (right scale, circles) of T2 Au/PS opal. The solid lines represent the calculated Bragg dispersion taking into account the wavelength dependence of the Au refractive index.

thickness or (ii) by increasing the core diameter. These calculations take into account the spherical shape of the core-shell structures. In our case the shape of the voids are changing with respect of the incident light, which can be interpreted as increasing of the core size along certain directions. An estimate of the red shift for a core-shell composite material containing a layer of 5 nm diameter Au particles to a core diameter increase of 60 nm would result in a shift in the transmission spectra from about 700 nm to 1100 nm. This calculation is in good agreement with the measured spectrum in the case discussed above, thus supporting our interpretation of the modification of the resonances due to the combined metallodielectric and latex photonic crystal.

CONCLUSIONS

To summarize, we studied and compared reflectance spectra of two different opal PhCs prepared from Au-PS core-shell spheres. Depending on the topology arising from the preparation method the optical behavior is different. In T1 opals the surface plasmon resonances are well separated and their relative intensities change regularly with angle of observation. This is attributed to the formation of well-defined and ordered oriented polyhedra in the opal voids. However, the "red" shift of plasmon resonances in these samples was not high enough to overlap with the diffraction resonance and, the Bragg dispersion remained unaffected. In T2 opals, with

higher NP density, the less ordered but denser aggregation of Au NPs results in a shift of the plasmon resonances towards the Bragg resonance. In this case, the interplay of the Bragg diffraction and wavelength dependence of the RI reversed the sign of the angular dispersion of the Bragg resonance. We propose that in order to achieve control over the PBG in core-shell metal-dielectric opals, these have to be highly impregnated with NPs and match closely the spectral range of the Bragg resonance with that of the plasmon resonance.

REFERENCES

[1] Busch, K. & John, S. (1998). *Phys. Rev. E*, *58*, 3896.
[2] Moroz, A. (1999). *Phys. Rev. Lett.*, *83*, 5274.
[3] Zhang, W. Y., Lei, X. Y., Wang, Z. L., Zheng, D. G., Tam, W. Y., Chan, C. T., & Sheng, P. (2000). *Phys. Rev. Lett.*, *84*, 2853.
[4] Oldenburg, S. J., Westcott, S. L., Averitt, R. D., & Halas, N. J. (1999). *J. Chem. Phys.*, *111*, 4729.
[5] Liang, Z., Susha, A. S., & Caruso, F. (2002). *Adv. Mater.*, *14*, 1160.
[6] Mie, G. (1908). *Ann. Phys.*, *25*, 377.
[7] Wang, Z., Chan, C. T., Zhang, W., Ming, N., & Sheng, P. (2001). *Phys. Rev. B.*, *64*, 113108.
[8] Balakirev, V. G., Bogomolov, V. N., Zhuravlev, V. V., Kumzerov, Y. A., Petranovskii, V. P., Romanov, S. G., & Samoilovich, L. A. (1993). *Crystallography Reports*, *38*, 348–353.
[9] Quinten, M. (2001). *Appl. Phys. B*, *73*, 245.
[10] Kreibig, U. & Vollmer, M. (1995). *Optical Properties of Metal Clusters*, Springer-Verlag: Berlin.
[11] Romanov, S. G., Maka, T., Sotomayor Torres, C. M., Müller, M., Zentel, R., Cassagne, D., Manzanares-Martinez, J., & Jouanin, C. (2001). *Phys. Rev. E*, *63*, 0566031.
[12] Palik, E. D. (1985). *Handbook of Optical Constants of Solids*, Academic Press: Boston.